Random-Defect Laser: Manipulating Lossy Two-Level Systems to Produce a Circuit with Coherent Gain

Yaniv J. Rosen,[1,2] Moe S. Khalil,[1,2] Alexander L. Burin,[3] and Kevin D. Osborn[1,4]
[1]*Laboratory for Physical Sciences, College Park, Maryland 20740, USA*
[2]*Department of Physics, University of Maryland, College Park, Maryland 20742, USA*
[3]*Department of Chemistry, Tulane University, New Orleans, Louisiana 70118, USA*
[4]*Joint Quantum Institute, College Park, Maryland 20742, USA*
(Received 11 January 2016; published 19 April 2016)

We demonstrate a laser using material defects known for deleterious microwave absorption in quantum computing. These defects are two-level atomic tunneling systems (TSs), which are manipulated using a uniform swept dc electric field and two ac pump fields. The swept field changes the TS energies. TSs first pass through degeneracy with pump photons, which invert (excite) them with a high probability using rapid adiabatic passage. Population inversion is accomplished in spite of a broad distribution of TS parameters. Afterwards the TSs are brought to degeneracy with the resonator where they emit photons. The emission is found to be dependent on individual cavity-TS interactions, and the narrowing linewidth at increasing photon occupancy indicates stimulated emission. Characterization with a microwave probe shows a transition from ordinary defect loss to negligible microwave absorption, and ultimately to coherent amplification. Thus, instead of absorbing microwave energy, the TSs can be tuned to reduce loss and even amplify signals.

DOI: 10.1103/PhysRevLett.116.163601

Nonlinear circuit elements are a key component in emerging technologies, and for superconducting devices including various photon detectors and quantum computing devices. For example, the superconducting transition [1] and the kinetic inductance of the superconductor [2,3] are both used for detector technologies. The Josephson junction is used in a wide range of new devices including superconducting qubits [4,5] and parametric amplifiers [6–8]. Additionally, when resonators have been coupled to superconducting [9,10] or semiconducting [11] qubits, effects such as artificial atom lasing [12–14] and arbitrary photon state preparation [9,15] can be demonstrated.

However, the development of superconducting qubits and detectors has been hindered by atomic tunneling systems (TSs) [16,17]. These TSs are known to arise within dielectric films and on the surfaces of the devices (due to surface oxides, fabrication contamination, etc.) [18–20]. The TSs cause decoherence in superconducting qubits [21], and for kinetic inductance detectors and resonators in general the TSs produce frequency noise [22]. To reduce the parasitic phenomena, most devices avoid certain materials [23] and reduce coupling to TSs using an optimized device geometry [24].

With awareness that a large set of devices are limited by TSs, we demonstrate that under certain conditions TSs can cause gain as well as loss. We use a swept bias electric field to change the TS energies and pump them with externally applied ac fields. At first, the TSs experience a classical pumping field, which can induce inversion. The TSs are then swept through degeneracy with the resonator. They couple strongly near resonance and can emit into the resonator. Similar to artificial-atom lasers, we use superconducting microwave resonators. However, our *sole* nonlinearity is created by the naturally occurring TSs within the capacitor dielectric. When the two-level TSs are pumped and swept in energy, the random ensemble becomes a lasing medium, which can produce coherent gain. The threshold of lasing agrees with a cavity quantum electrodynamics (cQED) model, constructed using previous measurements and the standard distribution of TS parameters. A probe tone is later added to demonstrate the transition between loss and coherent amplification (gain), which occurs after passing through an intermediate region of negligible microwave absorption.

TSs in dielectrics, and in amorphous materials in general, are described by a standard model with a distribution of double-well potentials. Each potential characterizes a TS with a tunneling energy Δ_0 and an asymmetry energy Δ [25,26]. For a microwave field at frequency ω_α and amplitude F_α applied to the dielectric of the resonator's capacitor, we can define a Rabi frequency for the TSs, $\Omega_\alpha = \Omega_{\alpha,0}(\Delta_0/\hbar\omega_\alpha)\cos\theta = (pF_\alpha/\hbar)(\Delta_0/\hbar\omega_\alpha)\cos\theta$, where θ is the angle between the TS dipole moment and the field. Here α denotes the different microwave fields, p for a pump field or r for the resonator field. Parallel to those microwave fields, a dc bias field $F_{\rm bias}$ is swept, causing a time-dependent TS asymmetry energy $\Delta(t) = \Delta(0) + 2pF_{\rm bias}(t)\cos\theta$. The sweep causes the energy of a TS, $E_{\rm TS} = \sqrt{\Delta(t)^2 + \Delta_0^2}$, to change in frequency at a rate of $v \equiv (1/\hbar)[d(E_{\rm TS})/dt] \simeq \pm v_0\sqrt{1-(\Delta_0/\hbar\omega_\alpha)^2}\cos\theta$,

where the maximum rate is $v_0 = 2p|\dot{F}_{\rm bias}|/\hbar$. Sweeping the TS frequency through ω_α can cause an adiabatic transition, $|g, n_\alpha\rangle \rightarrow |e, n_\alpha - 1\rangle$, with a probability of $P = 1 - \exp(-\pi\Omega_\alpha^2/2|v|)$, where $|g\rangle$ and $|e\rangle$ describe the TS states and n_α is the number of photons at frequency ω_α [27]. As found previously, despite the fact that increasing v_0 decreases the probability of inversion for a single TS, the energy exchanged with the field is greater due to a high rate of TSs passing through degeneracy with the field. Consequently, the power loss by TSs could only be increased by sweeping the bias [28]. In the current work we use pump fields to first invert TSs. Since the ramp rate v can be either positive or negative, two pumps, one at higher frequency than the resonator and one below it, are used to invert the TSs before they reach degeneracy with the resonator. Near the degeneracy, some TSs will coherently emit into the resonator through another adiabatic process, causing the quantum transition $|e, n_r\rangle \rightarrow |g, n_r + 1\rangle$ [29]. Figure 1(a) shows this transition schematically, as well as the counteracting process where the pump field does not invert the TS, and the TS absorbs a resonator photon instead.

The device uses four capacitors, each containing a SiN dielectric film with TSs [18], in an electrical bridge configuration, as shown in the schematic of Fig. 1(b). This allows a voltage bias to be applied to the same capacitors that are used for the ac resonance. With a standard single photon occupancy measurement [30], the resonator showed an internal quality factor $Q_i = 2500$ and a coupling quality factor $Q_C = 4800$.

The two pump fields are driven through the transmission line and detuned from resonance by ± 5 MHz in the data below. The device is in steady state operation when a constant voltage ramp is applied to the bias lead. A sawtooth waveform with a 100% duty cycle was used for the data shown. The voltage ramp rate was varied by changing the sawtooth period in a range between 10 μs and 100 ms, while keeping the amplitude constant. The TS relaxation time is short by comparison (TS relaxation time $T_1 \gtrsim 3$ μs [28]). Additionally, a 2 MHz filter used on the bias lead at the mixing chamber stage caused a relatively small transient time between waveform ramps. However, each data point was measured with a resolution bandwidth of 1–20 Hz and multiple ramping periods occurred for each point so any transient effects were averaged over.

As described above, we first measured the spectral emission while applying the pump tones and the bias sweep. A typical spectrum is shown in the inset of Fig. 1(c) where we used Q_c to convert the signal into a spectral photon density $(d\bar{n}/df)$. From an integration over the spectrum (above the noise floor) the mean number of photons in the resonator $\bar{n}$ was calculated and plotted as a function of pump voltage, the squares and diamonds in Fig. 1(c) (left axis). The pluses (right axis) show the FWHM of the emission, which is related to the coherence

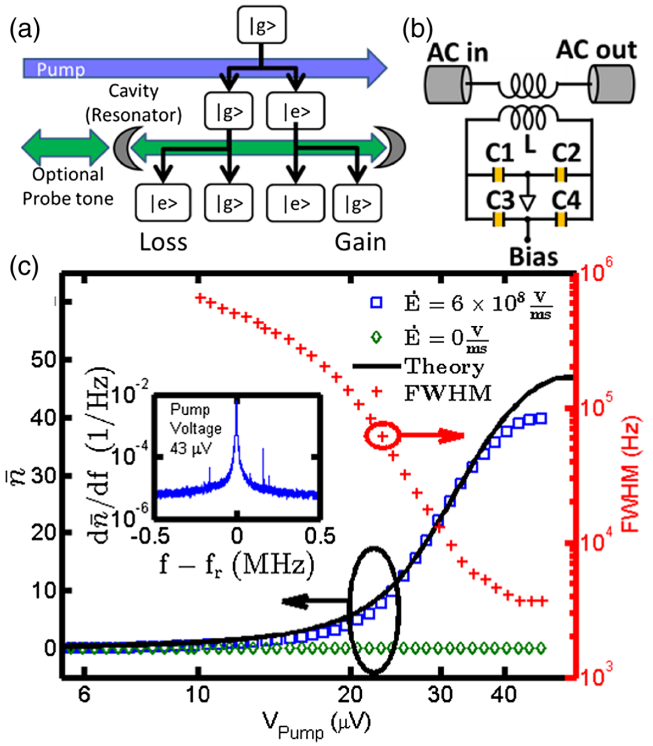

FIG. 1. (a) Diagram of two-level atomic tunneling system (TS) processes. TSs at low temperature start in $|g\rangle$, are pumped to $|e\rangle$, and can then emit into the resonator. (b) Circuit schematic of ac resonator decoupled from a dc bias line. TSs are contained in the capacitors (yellow). (c) Inset: Typical spectral photon density for the laser. A Lorentzian fit allows extraction of parameters for the main figure. Main figure: On the left-hand axis the photon number as a function of pump voltage is shown with (squares) and without (diamonds) a sweeping bias. The solid black line shows a theory generated without free parameters. On the right-hand axis the FWHM is shown (pluses) for the data with sweeping bias.

of the resonator field. Without a bias (green diamonds), no peak is detected and $\bar{n}$ remains near zero. When a sweeping bias is applied, and the pump voltage is increased, the number of photons in the resonator increases (blue squares) and the FWHM decreases (red pluses). When an emission peak is first observed, a Lorentzian fit gives a FWHM similar to the coupling, ~ 1 MHz $\cong (f_r/Q_C)$, which is expected for a spontaneous emission process. As the emission increases up to $\bar{n} = 40$, the FWHM decreases to 4 kHz.

To analyze the threshold we constructed a model [31] based on Ref. [27], which has added cQED fluctuations that were absent in an earlier work [29]. The model contains three primary probabilities for increasing the number of photons in the resonator. First, as shown in Fig. 1(a), a ground state TS has a probability of being inverted by the pumping field. Second, the TS has a probability of successfully traversing the frequencies between the pump and resonator without T_1 relaxation.

Finally, the TS has a probability of energy exchange with the resonator field, which at low photon numbers, $\bar{n} \lesssim 1$, is set by cQED fluctuations. This gain term, the loss due to ground state TSs, and the coupling loss of the resonator are analyzed using equations for power conservation to calculate the steady state photon number $\bar{n}$. The resulting theory curve is shown in Fig. 1(c). The inputs to the model were the measured values of Q_i and Q_c from the standard resonator analysis [30], along with the relaxation time $T_1 = 3\ \mu\text{s} \times (E_{\text{TS}}/\Delta_0)^2$ and the TS dipole moment of 7.9D, taken from Ref. [28]. The model, with no adjustable parameters, shows good qualitative agreement with the data, and good quantitative agreement up to $\bar{n} = 35$. This is likely because at high $\bar{n}$ we are no longer in the independent adiabatic Landau-Zener crossing regime. The lack of a sharp threshold in this device is due to the relatively low Q_c, which exceeds the intrinsic Q_i by only a factor of 2.

To further study the stimulated emission, we added a probe tone fixed on resonance (Fig. 2). At small input probe amplitudes ($V_{\text{rms}} = 1$ nV, compared to $V_{\text{pump,rms}} = 40\ \mu$V), the spectrum was identical to the case without the probe, and the FWHM of 4 kHz, was not affected. When a larger probe amplitude of $V_{\text{rms}} = 22$ nV was applied to the transmission line, TS emission detuned from the probe tone was reduced while the emission at the probe tone was increased. This shows that TSs undergo injection locking, where they preferentially emit coherently with the field. Therefore, the emission is stimulated rather than spontaneous.

We further investigated the stimulated process with a coherent probe of $V_{\text{rms}} = 26$ nV by measuring device transmission S_{21} for several different bias rates as a function of frequency. Figure 3(a) shows the magnitude of S_{21}, while Figs. 3(b) and 3(c) show the transmission quadratures, $\text{Re}(S_{21}) \equiv I$ and $\text{Im}(S_{21}) \equiv Q$, in an I-Q plot for different ramp rates. With a zero bias rate ($\dot{F}_{\text{bias}} = 0$), S_{21} shows a dip and a circular I-Q plot, which is characteristic of notch resonators with loss [30]. As expected, it does not change with the power of the pump tones because their influence is decoupled. As we increase the bias rate, the dip becomes deeper and narrower, indicating an increase in Q_i. This is caused by a decrease in power absorbed and an increase in TS emission. Similarly, the I-Q plot shows a circle with a larger radius. Increasing the rate further to $\dot{F}_{\text{bias}} = 6.4 \times 10^7$ V/ms actually reduces the dip seen in Fig 3(a); however, the I-Q plot shows a circle with an even larger radius. Resonant circles with $\text{Re}[S_{21}(f_r)] < 0$ imply that $Q_i < 0$, i.e., that the TSs are in the negative absorption regime [31].

At the next larger sweep rate, the bias produces a peak rather than a dip in $|S_{21}|$ as it is now amplifying the input signal due to the TS emission. The corresponding I-Q plot in Fig. 3(c) shows an ellipse rather than a circle, indicating that the material cannot be modeled with a single value of Q_i. This is expected because the TS emission is a nonlinear function of the photon number.

In this study, data were generally taken at 30 mK with the TSs in the ground state. However, to see the impact of the TS initial state on lasing we raised the temperature to 200 mK ($(2k_BT/\hbar\omega) \cong 1.76$) and confirmed that TS emission had been reduced significantly [see the gray dashed line in Fig. 3(a)]. Additionally, TSs must be inverted with high probability. The top curve of Fig. 3, where

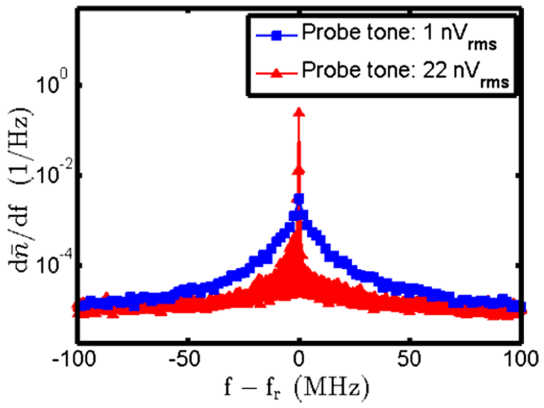

FIG. 2. Spectral photon density with a probe tone applied at the resonance frequency f_r. The squares (blue) show a spectrum resulting from a negligible probe. The FWHM is 4 kHz. The triangles (red) show the spectrum with a larger probe tone; it has a FWHM less than the measurement bandwidth (200 Hz). This behavior indicates injection locking.

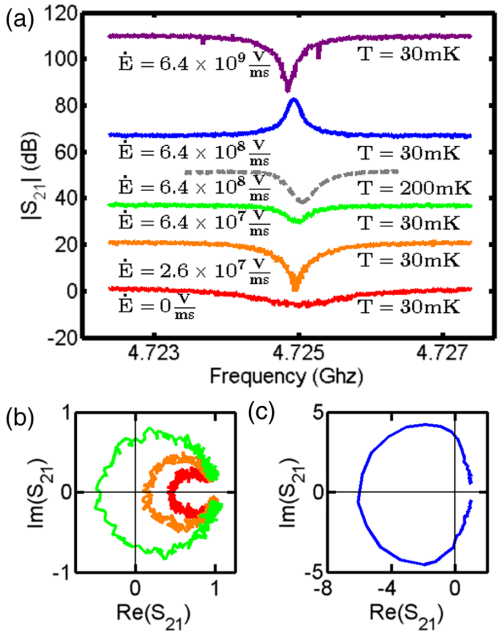

FIG. 3. (a) $|S_{21}|$ as a function of frequency for several different bias rates and two temperatures. (b) I-Q plots for the three lowest bias rates in (a) (circle radius increases with increasing bias). (c) I-Q plot for the next bias rate in (a) (blue solid line). Curves where $\text{Re}[S_{21}(f_r)] < 0$ can be interpreted as a negative absorption regime, even when $|S_{21}|$ does not show a peak.

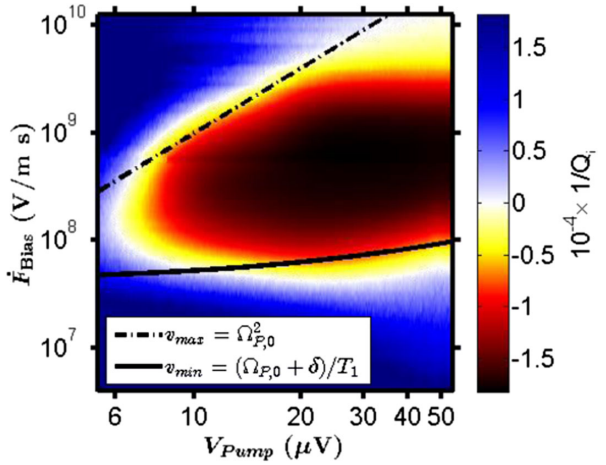

FIG. 4. $1/Q_i$ on resonance for different bias rates and pump powers, where negative values show negative absorption. The maximum ramp rate $v_{\max}$ (dashed line) shows the maximum rate for adiabatic inversion by the pump fields. The minimum ramp rate $v_{\min}$ (solid line) shows the minimum rate required for TSs to pass without relaxing (1) through the transition width for the inversion Ω_P and (2) through the detuning between the pump and resonator δ prior to relaxing.

$\dot{F}_{\mathrm{bias}} = 6.4 \times 10^9$ V/ms, shows no device gain because the TSs are traversing through the pumping field too quickly for inversion ($v \gg \Omega_p^2$).

We next extracted the absorption from $S_{21}(f_r)$. Figure 4 shows $(1/Q_i)$ as a function of the pump voltage and the bias rate. At $(1/Q_i) > 0$, the system is lossy. When $(1/Q_i) < 0$, the TSs are emitting into the resonator, but not enough power is generated in order to produce amplification. Amplification occurs for $-(1/Q_i) > (1/2Q_c) \sim 1 \times 10^{-4}$, as expected according to a general resonator model [31].

We compared the parameter space with the TS variables. The plot shows that negative absorption does not occur at very high or very low bias rates. For the inversion to take place, the TSs must traverse the pump tone adiabatically, meaning $v_0 < \Omega_{p,0}^2$. This puts an approximate upper limit on $\dot{F}_{\mathrm{bias}} \propto v_0$ shown as a dashed line in Fig. 4. The figure also shows evidence of a minimum bias rate for which lasing can occur. To invert, the TSs must change their frequency by the transition width Ω_p without relaxation. The time taken to invert, $\sim(\Omega_{p,0}/v_0)$, must be shorter than the decay time of the TSs, T_1. Once the TSs complete their inversion they must also traverse the $\delta = 2\pi \times 5$ MHz separation between the pump and resonance frequency so that $v_0 > (\delta/T_1)$ [31]. The positions of the cutoff lines confirm that the minimum T_1 is on the order of 3 μs, as found in this film type from previous work [28].

This laser shows that tunneling atomic systems are sufficiently controllable to create net gain with the random two-level state media. This allows a category of quantum-limited amplifiers made from superconductors and dielectric films laden with TSs, in contrast to superconducting parametric amplifiers that use either Josephson junctions [7,8] or the nonlinearity in kinetic inductors [6]. Additionally, our laser uses the same two levels for inversion and cavity interactions, while lasers generally use a third or fourth level for inversion. The dynamics are similar to micromasers [34–36], which give a rich set of coherent regimes related to the interaction times of the atoms with the cavity; however, because of the random nature of our media those regimes may be difficult to attain. Still, comparison with the micromaser may lead to future insights on the nature, distribution, and couplings of the TSs.

TSs are random two-level systems with a ubiquitous material origin. They cause microwave absorption, and thus decoherence in quantum computing devices. However, we demonstrated that a majority of the highest coupled TSs can be inverted. With the random media coupled to a resonator circuit, we demonstrated a laser made from random systems. By varying the system parameters, we transform the circuit from an initial defect loss regime, through a negligible microwave absorption regime, and finally to a coherent amplification regime. The threshold behavior for the laser was interpreted with a model that accounts for cavity quantum electrodynamics phenomena near single photon occupancy. Future experiments on the device could further explore the quantum to classical boundary of random two-level system excitations of lasers, as well as TS defect behavior in dielectrics. The negligible absorption state and the coherent amplification regimes may be particularly useful to reduce the deleterious effects of TSs in a broad range of devices, or to use the laser as a quantum-limited amplifier.

The authors would like to thank Rousko Hristov, Samaresh Guchhait, and Bahman Sarabi for useful conversations.

[1] B. Cabrera, R. M. Clarke, P. Colling, A. J. Miller, S. Nam, and R. W. Romani, Appl. Phys. Lett. **73**, 735 (1998).
[2] J. Gao, M. R. Vissers, M. O. Sandberg, F. C. S. da Silva, S. W. Nam, D. P. Pappas, D. S. Wisbey, E. C. Langman, S. R. Meeker, B. a. Mazin, H. G. Leduc, J. Zmuidzinas, and K. D. Irwin, Appl. Phys. Lett. **101**, 142602 (2012).
[3] P. K. Day, H. G. LeDuc, B. A. Mazin, A. Vayonakis, and J. Zmuidzinas, Nature (London) **425**, 817 (2003).
[4] M. H. Devoret and J. M. Martinis, Quantum Inf. Process. **3**, 163 (2004).
[5] M. P. Weides, J. S. Kline, M. R. Vissers, M. O. Sandberg, D. S. Wisbey, B. R. Johnson, T. A. Ohki, and D. P. Pappas, Appl. Phys. Lett. **99**, 262502 (2011).
[6] B. Ho Eom, P. K. Day, H. G. LeDuc, and J. Zmuidzinas, Nat. Phys. **8**, 623 (2012).
[7] M. A. Castellanos-Beltran and K. W. Lehnert, Appl. Phys. Lett. **91**, 083509 (2007).
[8] I. Siddiqi, R. Vijay, F. Pierre, C. M. Wilson, M. Metcalfe, C. Rigetti, L. Frunzio, and M. H. Devoret, Phys. Rev. Lett. **93**, 207002 (2004).

[9] M. Hofheinz, H. Wang, M. Ansmann, R. C. Bialczak, E. Lucero, M. Neeley, A. D. O'Connell, D. Sank, J. Wenner, J. M. Martinis, and A. N. Cleland, Nature (London) **459**, 546 (2009).
[10] M. Grajcar, S. H. W. van der Ploeg, A. Izmalkov, E. Ilichev, H.-G. Meyer, A. Fedorov, A. Shnirman, and G. Schön, Nat. Phys. **4**, 612 (2008).
[11] Y.-Y. Liu, K. D. Petersson, J. Stehlik, J. M. Taylor, and J. R. Petta, Phys. Rev. Lett. **113**, 036801 (2014).
[12] F. Chen, J. Li, A. D. Armour, E. Brahimi, J. Stettenheim, A. J. Sirois, R. W. Simmonds, M. P. Blencowe, and A. J. Rimberg, Phys. Rev. B **90**, 020506 (2014).
[13] J. Hauss, A. Fedorov, C. Hutter, A. Shnirman, and G. Schön, Phys. Rev. Lett. **100**, 037003 (2008).
[14] O. Astafiev, K. Inomata, A. O. Niskanen, T. Yamamoto, Y. A. Pashkin, Y. Nakamura, and J. S. Tsai, Nature (London) **449**, 588 (2007).
[15] M. Marthaler, G. Schön, and A. Shnirman, Phys. Rev. Lett. **101**, 147001 (2008).
[16] J. M. Martinis, K. B. Cooper, R. McDermott, M. Steffen, M. Ansmann, K. D. Osborn, K. Cicak, S. Oh, D. P. Pappas, R. W. Simmonds, and C. C. Yu, Phys. Rev. Lett. **95**, 210503 (2005).
[17] J. Gao, J. Zmuidzinas, B. A. Mazin, H. G. LeDuc, and P. K. Day, Appl. Phys. Lett. **90**, 102507 (2007).
[18] H. Paik and K. D. Osborn, Appl. Phys. Lett. **96**, 072505 (2010).
[19] A. D. O'Connell, M. Ansmann, R. C. Bialczak, M. Hofheinz, N. Katz, E. Lucero, C. McKenney, M. Neeley, H. Wang, E. M. Weig, A. N. Cleland, and J. M. Martinis, Appl. Phys. Lett. **92**, 112903 (2008).
[20] M. Sandberg, M. R. Vissers, J. S. Kline, M. Weides, J. Gao, D. S. Wisbey, and D. P. Pappas, Appl. Phys. Lett. **100**, 262605 (2012).
[21] W. D. Oliver and P. B. Welander, MRS Bull. **38**, 816 (2013).
[22] O. Noroozian, J. Gao, J. Zmuidzinas, H. G. LeDuc, B. A. Mazin, B. Young, B. Cabrera, and A. Miller, AIP Conf. Proc. **1185**, 148 (2009).
[23] J. B. Chang, M. R. Vissers, A. D. Corcoles, M. Sandberg, J. Gao, D. W. Abraham, J. M. Chow, J. M. Gambetta, M. Beth Rothwell, G. a. Keefe, M. Steffen, and D. P. Pappas, Appl. Phys. Lett. **103**, 012602 (2013).
[24] K. Geerlings, S. Shankar, E. Edwards, L. Frunzio, R. J. Schoelkopf, and M. H. Devoret, Appl. Phys. Lett. **100**, 192601 (2012).
[25] W. A. Phillips, Rep. Prog. Phys. **50**, 1657 (1987).
[26] P. W. Anderson, B. I. Halperin, and C. M. Varma, Philos. Mag. **25**, 1 (1972).
[27] A. L. Burin, M. S. Khalil, and K. D. Osborn, Phys. Rev. Lett. **110**, 157002 (2013).
[28] M. S. Khalil, S. Gladchenko, M. J. A. Stoutimore, F. C. Wellstood, A. L. Burin, and K. D. Osborn, Phys. Rev. B **90**, 100201 (2014).
[29] A. L. Burin, A. O. Maksymov, and K. D. Osborn, Supercond. Sci. Technol. **27**, 084001 (2014).
[30] M. S. Khalil, M. J. A. Stoutimore, F. C. Wellstood, and K. D. Osborn, J. Appl. Phys. **111**, 054510 (2012).
[31] See Supplemental Material at http://link.aps.org/supplemental/10.1103/PhysRevLett.116.163601, which includes Refs [32, 33]. For the threshold model, a discussion of the TS distribution, and a discussion of negative internal quality factors.
[32] M. Marthaler, J. Leppäkangas, and J. H. Cole, Phys. Rev. B **83**, 180505 (2011).
[33] B. T. H. Varcoe, S. Brattke, M. Weidinger, and H. Walther, Nature (London) **403**, 743 (2000).
[34] P. Filipowicz, J. Javanainen, and P. Meystre, Phys. Rev. A **34**, 3077 (1986).
[35] B.-G. Englert, arXiv:quant-ph/0203052.
[36] H. Walther, B. T. H. Varcoe, B.-G. Englert, and T. Becker, Rep. Prog. Phys. **69**, 1325 (2006).